A COMBINED FOURTH-ORDER COMPACT SCHEME WITH AN ACCELERATED MULTIGRID METHOD FOR THE ENERGY EQUATION IN SPHERICAL POLAR COORDINATES [*]

T. V. S. SEKHAR[†], R. SIVAKUMAR[‡], S. VIMALA[†], AND Y. V. S. S. SANYASIRAJU[§]

Abstract. A higher-order compact scheme is combined with an accelerated multigrid method to solve the energy equation in a spherical polar coordinate system. The steady forced convective heat transfer from a sphere which is under the influence of an external magnetic field is simulated. The convection terms in the energy equation are handled in a comprehensive way avoiding complications in the calculations. The angular variation of the Nusselt number and mean Nusselt number are calculated and compared with recent experimental results. Upon applying the magnetic field, a slight degradation of the heat transfer is found for moderate values of the interaction parameter N, and for high values of N an increase in the heat transfer is observed leading to a nonlinear behavior. The speedy convergence of the solution using the multigrid method and accelerated multigrid method is illustrated.

Key words. higher-order compact scheme, accelerated multigrid method, forced convection heat transfer, external magnetic field

AMS subject classifications. 65N06, 65N55, 35Q80

1. Introduction. The development of numerical methods for solving the Navier-Stokes equations is progressing from time to time in terms of accuracy, stability, and efficiency in using less CPU time and/or memory. It is well-known that at least second-order accurate solutions are required to capture flow phenomena such as boundary layer, vortices etc., while solving Navier-Stokes equations at high values of the Reynolds numbers (Re). The central difference scheme (CDS) causes nonphysical oscillations and lacks diagonal dominance in the resulting linear system. The first-order upwind difference approximation for convective terms and central differences for diffusion terms makes the finite difference scheme more stable due to artificial viscosity. Also, the diagonal dominance is assured for the linear system and so it can be solved easily using Point Gauss-Seidel or Line Gauss-Seidel, etc. As the convective terms are approximated by first-order upwind differences, the scheme is not second order accurate and may fail to capture the flow phenomena at high values of Re due to the dominance of convection. To achieve second-order accuracy, defect correction techniques are used [15, 29]. The second-order upwind methods are no better than the first-order upwind difference ones at high values of the flow parameters such as Re. All these methods require fine mesh grids to achieve grid independence or to get acceptable accuracy. Multigrid methods (which uses a sequence of coarser grids) are more popular in achieving fast convergence, which results in significant reduction of CPU time and also makes it possible to handle a huge number of mesh points to achieve acceptable accuracy. Notable contributions using the multigrid approach include articles by Ghia et al. [9], Fuchs and Zhao [8], Vanka [28], and Brandt [4]. Thompson [26] described a method which combines the multigrid method with automatic adaptive gridding to provide the basis of a stable solution strategy in Cartesian coordinate systems.

All the above methods may fail to capture the flow phenomena if the domain is too large such as in global ocean modeling and wide area weather forecasting applications. One ap-

proach to achieve accurate solutions with reduced computational costs in very large scale models and simulations is to use higher-order discretization methods. These methods use relatively coarse mesh grids to yield approximate solutions of comparable accuracy, relative to the lower-order discretization methods. The conventional higher-order finite difference methods contains ghost points and requires special treatment near the boundaries [2]. An exception has been found in the high-order finite difference schemes of compact type, which are computationally efficient and stable and give highly accurate numerical solutions [5, 10, 20]. To fully investigate the potential of using the fourth-order compact schemes for solving the Navier-Stokes equations, multigrid techniques are essential. These multigrid methods have been successfully used with first- and second-order finite difference methods. A preliminary investigation on combining the fourth-order compact schemes with multigrid techniques was made by Atlas and Burrage [1] for diffusion dominated flow problems.

Multigrid solution and accelerated multigrid solution methods with fourth-order compact schemes for solving convection-dominated problems are relatively new. Some attempts have been made in rectangular geometry [11, 12, 17, 21, 32, 33]. However, higher order compact schemes (HOCSs) are seldom applied to flow problems in curvilinear coordinate systems such as cylindrical and spherical polar coordinates except in [13, 14, 16, 19], where compact fourth-order schemes in cylindrical polar coordinates were developed. In particular, to the best of our knowledge, no work has been reported on high-order compact methods in spherical polar coordinate systems employing multigrid methods. The problem of heat transfer from a sphere which is under the influence of an external magnetic field is also new except for a few experimental results [3, 27, 31]. Fluid flow control using magnetic field (including dipole field) has a sound physical basis which may lead to a promising technology for better heat transfer control.

Hydromagnetic flows of electrically conducting fluids and its heat transfer have become more important in recent years because of many important applications including fusion technology. Early experimental exploration of a magnetic control of the heat transfer is reported by Boynton [3] in their study of magnetic heat transfer over a sphere. Uda et al. [27] experimentally studied MHD effects on the heat transfer of liquid Lithium flow in an annular channel. In their experimental study, Yokomine et al. [31] investigated heat transfer properties of aqueous potassium hydroxid solution ($Pr \approx 5$) and concluded that there is a degradation of the heat transfer with the magnetic field. In this paper, a HOCS is employed with a combination of accelerated multigrid technique to solve the energy equation in spherical polar coordinates. The forced convection heat transfer from a sphere which is under the influence of an external magnetic field is investigated.

2. Basic equations. The forced convective heat transfer problem is formulated as steady, laminar flow in axis-symmetric spherical polar coordinates. The center of the sphere is chosen at the origin and the flow is symmetric about $\theta = \pi$ (upstream) and $\theta = 0^o$ (downstream). The fluid is considered to be incompressible, viscous, and electrically conducting. A uniform stream from infinity, U_∞, is imposed from left to right at far distances from the sphere. The magnetic Reynolds number is assumed to be small so that the induced magnetic field can be neglected and a constant magnetic field

$$(2.1) \qquad\qquad H = (-\cos\theta,\ \sin\theta,\ 0)$$

is imposed opposite to the flow. The governing equations are the Navier-Stokes equations and Maxwell's equations which are expressed in non-dimensional form as follows:

$$\nabla \cdot \mathbf{q} = 0$$

$$(\mathbf{q} \cdot \nabla)\mathbf{q} = -\nabla p + \frac{2}{Re}\nabla^2 \mathbf{q} + N[\mathbf{J} \times \mathbf{H}]$$

(2.2) $$\mathbf{J} = \nabla \times \mathbf{H} = \mathbf{E} + \mathbf{q} \times \mathbf{H}$$

$$\nabla \cdot \mathbf{H} = 0$$

$$\nabla \times \mathbf{E} = 0,$$

where $\mathbf{q}$ is the fluid velocity, $\mathbf{H}$ is the magnetic field, p is the pressure, $\mathbf{E}$ is the electric field, $\mathbf{J}$ is the current density and N is the interaction parameter defined as $N = \sigma H_\infty^2 a / \rho U_\infty$. Here σ and ρ are the electric conductivity and the density of the fluid and a is the radius of the sphere. $Re = 2aU_\infty/\nu$ is the Reynolds number based on the diameter $(2a)$ of the sphere. In order to have fine resolution near the surface of the sphere, we have used the transformation $r = e^\xi$ along the radial direction, which provides the solution in the non-uniform physical plane while keeping the uniform grid in the computational plane as shown in Figure 2.1. The fluid motion is described by radial and transverse components of the velocity $(q_r,\ q_\theta)$ in a plane through the axis of symmetry, which are obtained by dividing the corresponding dimensional components by the main-stream velocity U_∞. The velocity components are expressed in terms of a dimensionless stream function $\psi(\xi, \theta)$ such that the equation of continuity $\nabla \cdot \mathbf{q} = 0$ is satisfied. The velocity components q_r and q_θ are as follows:

(2.3) $$q_r = \frac{e^{-2\xi}}{\sin\theta}\frac{\partial\psi}{\partial\theta}, \qquad\qquad q_\theta = -\frac{e^{-2\xi}}{\sin\theta}\frac{\partial\psi}{\partial\xi}.$$

They are obtained by solving the momentum equation expressed in the vorticity-stream function formulation. The velocity field is obtained by solving equations (2.1–2.3) using a finite difference based multigrid method followed by a defect correction technique developed by Sekhar et al. [24]. The grid independent velocity components obtained from (2.1–2.3) over a high resolution grid 512×512 are used to solve the energy equation. If the physical properties of the fluid are assumed to be constant and the internal generation of heat by friction is neglected, the energy equation is given by

(2.4) $$\frac{\partial^2\Theta}{\partial\xi^2} + \frac{\partial\Theta}{\partial\xi} + \cot\theta\frac{\partial\Theta}{\partial\theta} + \frac{\partial^2\Theta}{\partial\theta^2} = \frac{RePr}{2}\frac{e^{-\xi}}{\sin\theta}\left(\frac{\partial\psi}{\partial\theta}\frac{\partial\Theta}{\partial\xi} - \frac{\partial\psi}{\partial\xi}\frac{\partial\Theta}{\partial\theta}\right),$$

where $\Theta(\xi,\ \theta)$ is the non-dimensionalized temperature, defined by subtracting the main-flow temperature Θ_∞ from the temperature and dividing by $\Theta_s - \Theta_\infty$. Pr is the Prandtl number defined as the ratio between kinematic viscosity ν and thermal diffusivity κ. The boundary conditions for the temperature are $\Theta = 1$ on the surface of the sphere, $\Theta \to 0$ as $\xi \to \infty$, and $\frac{\partial\Theta}{\partial\theta} = 0$ along the axis of symmetry. The numerical scheme used to solve the equations (2.1–2.3) is described in [24], and the details of the fourth-order compact scheme to solve equation (2.4) are given in the following section.

3. Fourth-order scheme with the MG method. Both the fluid motion and the temperature field are axially symmetric and hence all computations have been performed only in one of the symmetric region. The discretization of the governing equation (2.4) in the symmetric region is done using the compact stencil. By combining the convection terms $\frac{\partial\psi}{\partial\theta}\frac{\partial\Theta}{\partial\xi}$ and $\frac{\partial\psi}{\partial\xi}\frac{\partial\Theta}{\partial\theta}$ on the right-hand side of equation (2.4) with the terms $\frac{\partial\Theta}{\partial\xi}$ and $\cot\theta\frac{\partial\Theta}{\partial\theta}$, respectively, we obtain

(3.1) $$-\frac{\partial^2\Theta}{\partial\xi^2} - \frac{\partial^2\Theta}{\partial\theta^2} + u\frac{\partial\Theta}{\partial\xi} + v\frac{\partial\Theta}{\partial\theta} = 0,$$
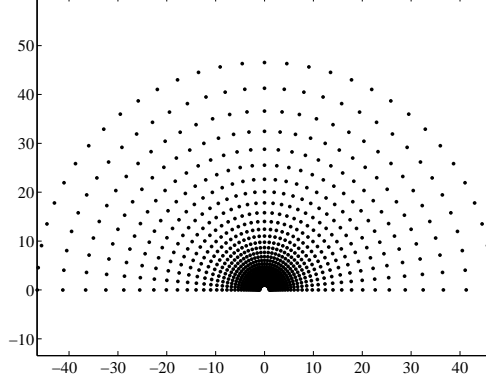
FIG. 2.1. *The grid points of the non-uniform grid in which the final solution is obtained.*

where

$$(3.2) \qquad u = \frac{RePr}{2}e^{\xi}q_r - 1, \qquad v = \frac{RePr}{2}e^{\xi}q_{\theta} - \cot\theta.$$

The velocity components q_r and q_{θ} in equation (3.2) are obtained using a usual fourth-order approximations from the stream function ψ. Applying standard central difference operators to equation (3.1) gives

$$(3.3) \qquad -\delta_{\xi}^2\Theta_{i,j} - \delta_{\theta}^2\Theta_{i,j} + u_{i,j}\delta_{\xi}\Theta_{i,j} + v_{i,j}\delta_{\theta}\Theta_{i,j} - \tau_{i,j} = 0.$$

The truncation error of equation (3.3) is given by

$$(3.4) \qquad \tau_{i,j} = \left[2\left(\frac{h^2}{12}u\frac{\partial^3\Theta}{\partial\xi^3} + \frac{k^2}{12}v\frac{\partial^3\Theta}{\partial\theta^3}\right) - \left(\frac{h^2}{12}\frac{\partial^4\Theta}{\partial\xi^4} + \frac{k^2}{12}\frac{\partial^4\Theta}{\partial\theta^4}\right)\right]_{i,j} + O(h^4, k^4),$$

where h and k are the grid spacings ($h \neq k$) in the radial and angular directions, respectively. From equation (3.1), we get

$$\frac{\partial^3\Theta}{\partial\xi^3} = -\frac{\partial^3\Theta}{\partial\xi\partial\theta^2} + u\frac{\partial^2\Theta}{\partial\xi^2} + \frac{\partial u}{\partial\xi}\frac{\partial\Theta}{\partial\xi} + v\frac{\partial^2\Theta}{\partial\xi\partial\theta} + \frac{\partial v}{\partial\xi}\frac{\partial\Theta}{\partial\theta},$$

$$\frac{\partial^4\Theta}{\partial\xi^4} = -\frac{\partial^4\Theta}{\partial\xi^2\partial\theta^2} + v\frac{\partial^3\Theta}{\partial\xi^2\partial\theta} - u\frac{\partial^3\Theta}{\partial\xi\partial\theta^2} + \left(2\frac{\partial v}{\partial\xi} + uv\right)\frac{\partial^2\Theta}{\partial\xi\partial\theta}$$
$$+ \left(2\frac{\partial u}{\partial\xi} + u^2\right)\frac{\partial^2\Theta}{\partial\xi^2} + \left(\frac{\partial^2 u}{\partial\xi^2} + u\frac{\partial u}{\partial\xi}\right)\frac{\partial\Theta}{\partial\xi}$$
$$+ \left(\frac{\partial^2 v}{\partial\xi^2} + u\frac{\partial v}{\partial\xi}\right)\frac{\partial\Theta}{\partial\theta},$$

$$\frac{\partial^3\Theta}{\partial\theta^3} = -\frac{\partial^3\Theta}{\partial\xi^2\partial\theta} + u\frac{\partial^2\Theta}{\partial\xi\partial\theta} + \frac{\partial u}{\partial\theta}\frac{\partial\Theta}{\partial\xi} + v\frac{\partial^2\Theta}{\partial\theta^2} + \frac{\partial v}{\partial\theta}\frac{\partial\Theta}{\partial\theta},$$

$$\frac{\partial^4\Theta}{\partial\theta^4} = -\frac{\partial^4\Theta}{\partial\xi^2\partial\theta^2} + u\frac{\partial^3\Theta}{\partial\xi\partial\theta^2} - v\frac{\partial^3\Theta}{\partial\xi^2\partial\theta} + \left(2\frac{\partial u}{\partial\theta} + uv\right)\frac{\partial^2\Theta}{\partial\xi\partial\theta}$$
$$+ \left(2\frac{\partial v}{\partial\theta} + v^2\right)\frac{\partial^2\Theta}{\partial\theta^2} + \left(\frac{\partial^2 u}{\partial\theta^2} + v\frac{\partial u}{\partial\theta}\right)\frac{\partial\Theta}{\partial\xi}$$
$$+ \left(\frac{\partial^2 v}{\partial\theta^2} + v\frac{\partial v}{\partial\theta}\right)\frac{\partial\Theta}{\partial\theta}.$$

A substitution in equation (3.4) and hence in (3.3) yields

$$
- e_{i,j}\delta_\xi^2\Theta_{i,j} - f_{i,j}\delta_\theta^2\Theta_{i,j} + g_{i,j}\delta_\xi\Theta_{i,j} + o_{i,j}\delta_\theta\Theta_{i,j}
$$
$$
- \frac{h^2 + k^2}{12}\big(\delta_\xi^2\delta_\theta^2\Theta_{i,j} - u_{i,j}\delta_\xi\delta_\theta^2\Theta_{i,j} - v_{i,j}\delta_\xi^2\delta_\theta\Theta_{i,j}\big) + w_{i,j}\delta_\xi\delta_\theta\Theta_{i,j} = 0,
$$

where the coefficients $e_{i,j}$, $f_{i,j}$, $g_{i,j}$, $o_{i,j}$ and $w_{i,j}$ are given by

$$
e_{i,j} = 1 + \frac{h^2}{12}\left(u_{i,j}^2 - 2\delta_\xi u_{i,j}\right)
$$
$$
f_{i,j} = 1 + \frac{k^2}{12}\left(v_{i,j}^2 - 2\delta_\theta v_{i,j}\right)
$$
$$
g_{i,j} = u_{i,j} + \frac{h^2}{12}\left(\delta_\xi^2 u_{i,j} - u_{i,j}\delta_\xi u_{i,j}\right) + \frac{k^2}{12}\left(\delta_\theta^2 u_{i,j} - v_{i,j}\delta_\theta u_{i,j}\right)
$$
$$
o_{i,j} = v_{i,j} + \frac{h^2}{12}\left(\delta_\xi^2 v_{i,j} - u_{i,j}\delta_\xi v_{i,j}\right) + \frac{k^2}{12}\left(\delta_\theta^2 v_{i,j} - v_{i,j}\delta_\theta v_{i,j}\right)
$$
$$
w_{i,j} = \frac{h^2}{6}\delta_\xi v_{i,j} + \frac{k^2}{6}\delta_\theta u_{i,j} - \left(\frac{h^2 + k^2}{12}\right)u_{i,j}v_{i,j},
$$

and the two-dimensional cross derivative δ operators on a uniform anisotropic mesh ($h \neq k$) are given by

$$
\delta_\xi\delta_\theta\Theta_{i,j} = \frac{1}{4hk}\left(\Theta_{i+1,j+1} - \Theta_{i+1,j-1} - \Theta_{i-1,j+1} + \Theta_{i-1,j-1}\right)
$$
$$
\delta_\xi^2\delta_\theta\Theta_{i,j} = \frac{1}{2h^2k}\left(\Theta_{i+1,j+1} - \Theta_{i+1,j-1} + \Theta_{i-1,j+1} - \Theta_{i-1,j-1} - 2\Theta_{i,j+1} + 2\Theta_{i,j-1}\right)
$$
$$
\delta_\xi\delta_\theta^2\Theta_{i,j} = \frac{1}{2hk^2}\left(\Theta_{i+1,j+1} - \Theta_{i-1,j+1} + \Theta_{i+1,j-1} - \Theta_{i-1,j-1} + 2\Theta_{i-1,j} - 2\Theta_{i+1,j}\right)
$$
$$
\delta_\xi^2\delta_\theta^2\Theta_{i,j} = \frac{1}{h^2k^2}\big(\Theta_{i+1,j+1} + \Theta_{i+1,j-1} + \Theta_{i-1,j+1} + \Theta_{i-1,j-1}
$$
$$
- 2\Theta_{i,j+1} - 2\Theta_{i,j-1} - 2\Theta_{i+1,j} - 2\Theta_{i-1,j} + 4\Theta_{i,j}\big).
$$

For evaluating boundary conditions along the axis of symmetry, the derivative $\frac{\partial\Theta}{\partial\theta}$ is approximated by a fourth-order forward difference along $\theta = 0$ (i.e., $j = 1$) and a fourth-order backward difference along $\theta = \pi$ (or $j = m + 1$) as follows:

$$
\Theta(i,\ 1) = \frac{1}{25}\left[48\Theta(i,\ 2) - 36\Theta(i,\ 3) + 16\Theta(i,\ 4) - 3\Theta(i,\ 5)\right]
$$
$$
\Theta(i,\ m + 1) = \frac{1}{25}\left[48\Theta(i,\ m) - 36\Theta(i,\ m - 1) + 16\Theta(i,\ m - 2) - 3\Theta(i,\ m - 3)\right].
$$

The algebraic system of equations obtained using the fourth-order compact scheme described as above is solved using a multigrid scheme with coarse grid correction. Point Gauss-Seidel relaxation is used as pre-smoothers and post-smoothers. Please note that as the grid independent solutions of the flow (like ψ and ω) are obtained from the finest grid of 512×512, the same finest grid is used when solving the heat transfer equation although such a high resolution grid is not necessary. The coarser grids used are 256×256, 128×128, 64×64 and the coarsest grid 32×32. The injection operator and 9-point prolongation operators are used to move from finer to coarser and coarser to finer grids, respectively, [9]. For a two-grid problem, to solve $\mathcal{L}u = f$, one iteration implies the following steps:

1. Let the initial solution be $u_\circ$ on the finest grid.
2. Apply Point Gauss Seidel iterations on $u_\circ$ on the finest grid a few times as pre-smoother to get an approximate solution u_1.
3. Calculate the residue r on the finest grid, $r = f - \mathcal{L}_f u_1$.
4. To get the residue on a coarser grid r_c, restrict the residue r from the finer to the coarser grid and then multiply with a residual scaling parameter β, that is, $r_c = \beta \mathcal{R} r$. Here $\mathcal{R}$ represents the restriction operator.
5. Setup the error equation $\mathcal{L}_c e_c = r_c$ on the coarser grid and solve for the error e using the Point Gauss Seidel method. This gives the error on the coarser grid.
6. To get the error e on the finer grid, prolongate the error e_c to the finer grid and then multiply with a residual weighting parameter α. Add this error e to the solution u_1 obtained in Step 2 to get an improved solution u_2. That is, $u_2 = u_1 + \alpha \mathcal{P} e_c$, where $\mathcal{P}$ is the 9-point prolongation operator.
7. Perform a few Point Gauss-Seidel iterations on the solution u_2 on the finer grid to obtain a much better solution u_3.
8. Consider u_3 as $u_\circ$ and go to Step 2.

The Steps 1–8 above constitute one iteration of the two-grid problem. The iterations are continued until the norm of the dynamic residuals is less than 10^{-5}. In the algorithm given above, if $\alpha = \beta = 1$, then it is a standard two-grid method with coarse grid correction. The parameters α and β are used to accelerate the convergence rate. In this study, we used values with $0 < \alpha < 2$ and $0 < \beta < 2$.

4. Results and discussion. The higher-order compact scheme combined with an accelerated multigrid method introduced in Section 3 is applied to the problem of a heated sphere which is immersed in an incompressible, viscous, and electrically conducting fluid. An external magnetic field is applied in the opposite direction of the uniform stream. In this study, mainly two flow parameters, $Re = 5$ and $Re = 40$, are considered, in which the earlier has no boundary layer separation while the latter has a separation. The results are discussed for the range of N for $0 \le N \le 8$ and the Prandtl numbers $Pr = 0.065, 0.73, 1, 2, 5, 8$. The local Nusselt number $Nu(\theta)$ and the mean Nusselt number N_m are calculated as follows:

$$(4.1) \qquad Nu(\theta) = \frac{2aq(\theta)}{k(\Theta_s - \Theta_\infty)} = -2 \left(\frac{\partial \Theta}{\partial \xi} \right)_{\xi=0}$$

and

$$(4.2) \qquad N_m = - \int_0^\pi \left(\frac{\partial \Theta}{\partial \xi} \right)_{\xi=0} \sin \theta \, d\theta.$$

In equations (4.1) and (4.2) the derivative $\frac{\partial \Theta}{\partial \xi}$ is approximated by usual fourth-order forward finite differences and the integral is evaluated using the Simpson's rule.

In the absence of a magnetic field ($N = 0$) the basic hydrodynamic problem is equivalent to the steady viscous flow around a sphere. Therefore, for $N = 0$, the developed scheme is validated with the available theoretical results (Table 4.1) for $Re = 5$ and 40. It is clear from the table that the present results agree well with the numerical results of Dennis [6] with a variation of 0.35 percent and recent results of Feng and Michaelides [7] with a variation of 0.20–4.78 percent. The results also agree with experimental results of Ranz and Marshall [22, 23] with a variation of 0.47–11.21 percent and Whitaker [30] with a variation of 3.06–6.75 percent.

The simulations have been carried out over 32×32, 64×64, 128×128, 256×256, and 512×512 grids, and the mean Nusselt number for $Re = 5$ and 40 for selected values of Pr

TABLE 4.1
Comparison of the mean Nusselt number with results in literature in the absence of the magnetic field.

	N_m for $Re = 5$		N_m for $Re = 40$	
	$Pr = 0.73$	$Pr = 5$	$Pr = 0.73$	$Pr = 5$
Present simulation	2.8518	4.3101	5.0449	8.6987
Ranz & Marshall (1952)	3.2080	4.2942	5.4168	8.4889
Whitaker (1972)	2.9433	4.0366	4.8493	8.1518
Dennis (1973)	2.86	—	—	—
Feng & Michaelides (2000)	2.7250	4.3460	5.0545	8.7700

and N are presented in Tables 4.2, 4.3, 4.4, and 4.5. It is clear from these tables that (i) the solutions obtained from the present numerical scheme exhibit grid independence, and (ii) it is possible to obtain grid independence in the smaller 64×64 grid for low Prandtl numbers Pr. For higher values of Pr, a grid finer than 64×64 but less than 128×128 is necessary for grid independence. Clearly, solutions obtained from high resolution grids such as 256×256 and 512×512 are not required as mentioned in the previous section.

TABLE 4.2
Effect of grid size on the results for $Re = 5$ and $Pr = 0.73$.

N	N_m				
	32×32	64×64	128×128	256×256	512×512
0.5	2.849	2.850	2.850	2.850	2.850
1	2.858	2.859	2.859	2.859	2.859
3	2.885	2.886	2.886	2.886	2.886
5	2.900	2.901	2.901	2.901	2.901
8	2.915	2.917	2.917	2.917	2.917

TABLE 4.3
Effect of grid size on the results $Re = 40$ and $Pr = 0.73$.

N	N_m				
	32×32	64×64	128×128	256×256	512×512
0.5	4.928	4.982	4.986	4.986	4.986
1	4.913	4.962	4.965	4.965	4.965
3	4.920	4.964	4.967	4.967	4.967
5	4.948	4.994	4.997	4.998	4.998
8	5.004	5.053	5.057	5.057	5.057

The fourth-order compact scheme is combined with an accelerated multigrid technique to achieve fast convergence so that CPU time can be minimized. Although multigrid methods are well established with first- and second-order discretization methods, their combination with higher-order compact schemes are not found much in the literature. To study the effect of the multigrid method and accelerated multigrid method on the convergence of the Point Gauss-Seidel iterative method while solving the resulting algebraic system of equations, the

TABLE 4.4
Effect of grid size on the results $Re = 5$ and $N = 2$.

Pr	N_m				
	32×32	64×64	128×128	256×256	512×512
0.065	2.142	2.142	2.142	2.142	2.142
0.73	2.873	2.874	2.874	2.874	2.874
1	3.051	3.053	3.053	3.053	3.053
2	3.530	3.536	3.536	3.536	3.536
5	4.369	4.398	4.400	4.400	4.400
8	4.899	4.962	4.965	4.965	4.965

TABLE 4.5
Effect of grid size on the results $Re = 40$ and $N = 2$.

Pr	N_m				
	32×32	64×64	128×128	256×256	512×512
0.065	2.780	2.781	2.781	2.781	2.781
0.73	4.910	4.955	4.957	4.958	4.958
1	5.330	5.403	5.408	5.408	5.408
2	6.400	6.572	6.589	6.590	6.590
5	8.510	8.549	8.640	8.644	8.644
8	10.464	9.763	9.961	9.970	9.970

TABLE 4.6
Comparison of CPU times (in hours) with second-order accurate scheme.

$Grid$	CPU time in hours	
	Second-order	HOCS
64×64	0.00083	0.00027
128×128	0.01055	0.00277
256×256	0.1575	0.07527
512×512	2.9108	2.2291
$32^2 - 128^2$	—	0.0011*
$32^2 - 512^2$	1.29*	0.1158

∗ CPU time on achieving grid independence

solution is obtained from different multigrids starting with five grids 32×32, 64×64, 128×128, 256×256, and 512×512, and by omitting each coarser grid until it reaches the single grid 512×512. This experiment is done with $Re = 40$, $Pr = 0.73$ and four values of interaction parameters, 0, 0.5, 2 and 7. The simulations are also made for $Re = 40$, $N = 2$ and for selected values of Pr, 0.73, 2 and 5. The computations are carried out on an AMD quad core Phenom-II X4 965 (3.4 GHz) desktop computer. The number of iterations and CPU time (in hours) taken for different multigrids and single grid are illustrated in Figures 4.1 and 4.2. From these figures it is clear that the multigrid method with coarse grid correction is very effective in enhancing the convergence rate of the solutions. It enhances the convergence rate

at least 94 percent in comparison with a single grid. The accelerated multigrid technique further enhances the convergence rate by reducing 21 percent of the time taken by multigrid (5 grids). In this study, the acceleration parameters which are found suitable for enhancement of the convergence rate for one value of Pr, in the absence of the magnetic field, is suitable for all values of the non-zero interaction parameters. The results are also obtained for some parameters using a second-order accurate scheme combined with the multigrid method [24]. The CPU time (in hours) taken for both the methods in each grid as well as the multigrid are tabulated in Table 4.6. It can be noted from the table that HOCS is more computationally efficient when compared to second-order accurate scheme in each grid as well as when it is combined with the multigrid method.
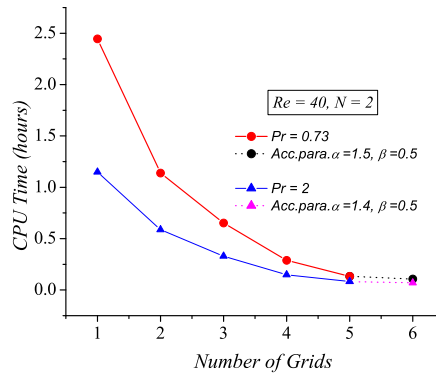
FIG. 4.1. *Effect of the multigrid and acceleration parameter on the convergence factor for $Re = 40$ and $N = 2$, where the range between 5 to 6 on the x-axis indicates 5 grids with acceleration parameters $\alpha = 1.5$, $\beta = 0.5$ for $Pr = 0.73$ and $\alpha = 1.4$, $\beta = 0.5$ for $Pr = 2$.*
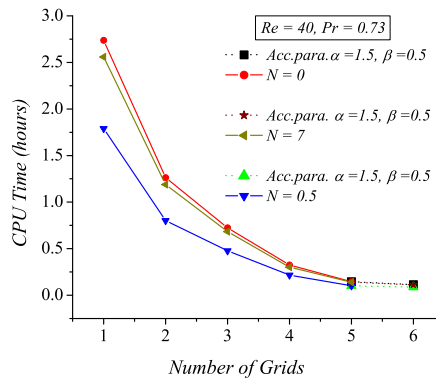
FIG. 4.2. *Effect of the multigrid and acceleration parameter on convergence factor $Re = 40$ and $Pr = 0.73$, where the range between 5 to 6 on the x-axis indicates 5 grids with acceleration parameters $\alpha = 1.5$, $\beta = 0.5$.*

4.1. Local and mean Nusselt numbers. The angular variation of the local Nusselt number Nu on the surface of the sphere for different Prandtl numbers and for different interaction parameters are presented in Figures 4.3, 4.4, and 4.5. In the absence of a magnetic
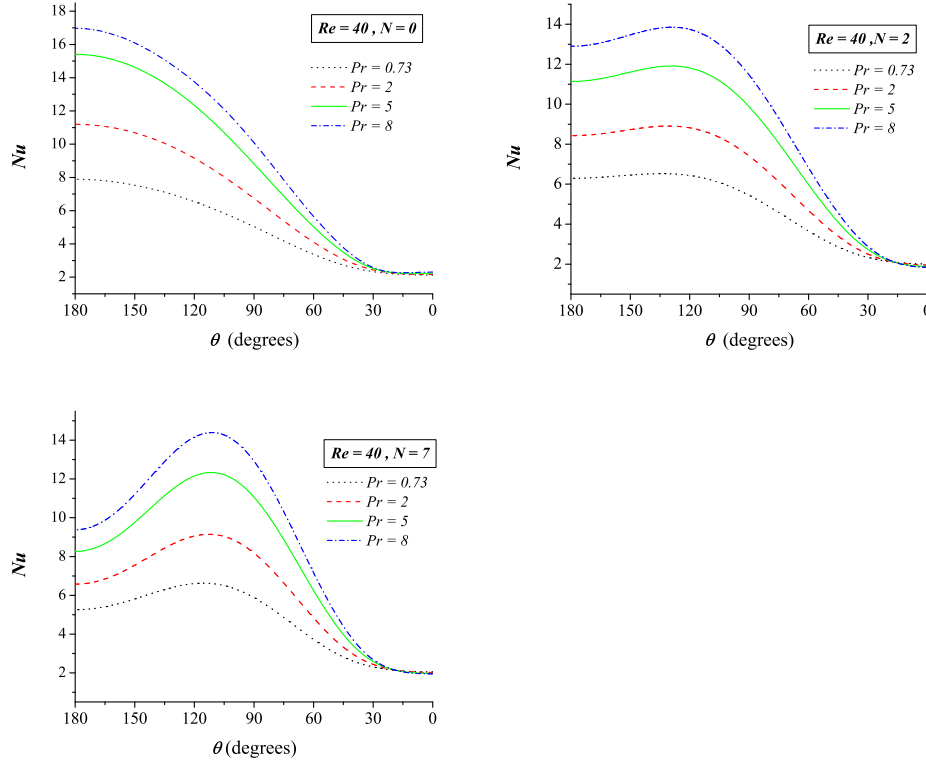
FIG. 4.3. *Angular variation of the Nusselt number for $Re = 40$ when $N = 0$, $N = 2$ and $N = 7$.*

field, it is found that the local Nusselt number decreases along the surface of the sphere for Reynolds numbers $Re = 5$ [6] and for $Re = 40$. In the upstream region (Figures 4.4, 4.5), the viscous boundary layer thickens with the application of the magnetic field. All the curves in Figure 4.5 meet at one critical point after which an inverse effect is exhibited, that is, the boundary layer gets thinner with the magnetic field. The curves meet once again in the far downstream. These features are attributed to changes in the radial and transverse velocity gradients of the fluid, which resulted due to the application of the magnetic field to the flow [25]. The applied magnetic field brings changes in the local Nusselt number. While studying the dependence of Nu on Pr, when an external magnetic field is not present, the maximum heat transfer takes place near the front stagnation point $\theta = \pi$ (Figure 4.3), whereas, when the magnetic field is increased, the peak heat transfer region is shifted towards $\theta = \pi/2$. Irrespective of the magnetic field, when Pr is increased, the local Nusselt number increased along the surface of the sphere. However, the heat transfer rate of a fluid with higher Pr is affected more by the external magnetic field when compared to a fluid with lower Pr. The higher values of Nu for higher Re, as seen from Figures 4.4 and 4.5, is as expected, since fluids with larger Reynolds number indicate dominant convection, wherein the viscous and thermal boundary layers get thinner with growing Re. When these local values of the heat flux is surface-averaged over the sphere, we get the mean Nusselt number N_m. From Figure 4.6, we observe that there is a degradation in the mean Nusselt number when $0 \leq N \leq 2$ beyond which it increases leading to a non-linear behavior. This observation is in line with
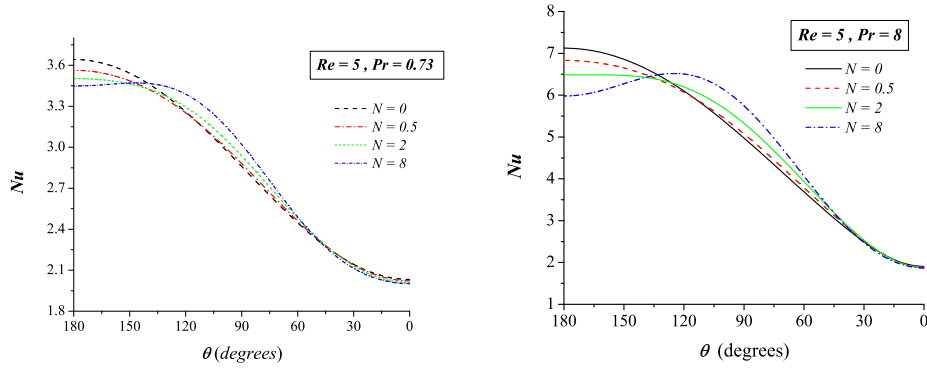
FIG. 4.4. *Angular variation of the Nusselt number for $Re = 5$ when $Pr = 0.73$ and $Pr = 8$.*
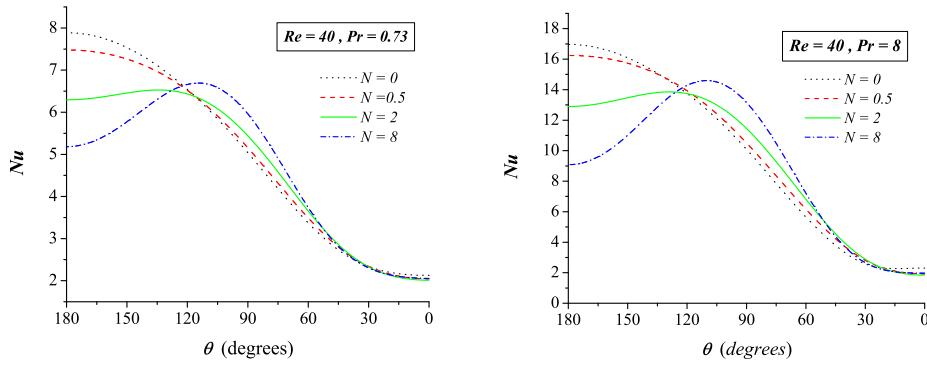
FIG. 4.5. *Angular variation of the Nusselt number for $Re = 40$ when $Pr = 0.73$ and $Pr = 8$.*

the recent experimental findings of Uda et al. [27] and Yokomine et al. [31]. In particular, to compare our results with the recent experimental results of Yokomine et al. at low values of N up to 0.1, simulations are made with KOH solution with $Pr = 5$ for $Re = 5$ and 40, and the mean Nusselt number is presented in Figure 4.7. The degradation of the heat transfer found in this study, at low values of N, is also in agreement with experimental results [31]. The increased N_m with Pr, as observed here, is in agreement with [18] in their study without magnetic field.

5. Conclusions. A higher-order compact scheme is combined with an accelerated multigrid method in spherical polar coordinates to simulate the steady forced convective heat transfer from a sphere under the influence of an external magnetic field. The speedy convergence of the solution using the multigrid method and accelerated multigrid method is illustrated. The computational efficiency of the higher-order compact scheme over second-order accurate scheme is presented. The angular variation of the Nusselt number and mean Nusselt number are calculated and compared with recent experimental results. Upon applying the magnetic field, a slight degradation of the heat transfer is found for moderate values of the interaction parameter N, and for high values of N, an increase in the heat transfer is observed, leading to nonlinear behavior.
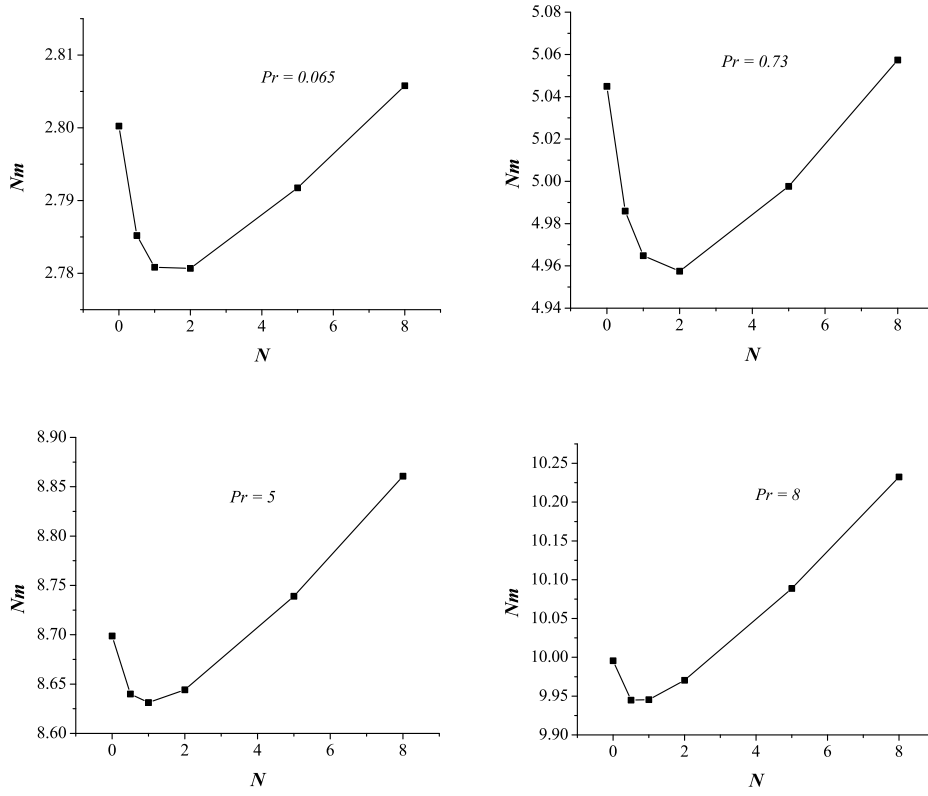
FIG. 4.6. *Variation of the mean Nusselt number N_m with magnetic field N for different Pr when $Re = 40$.*
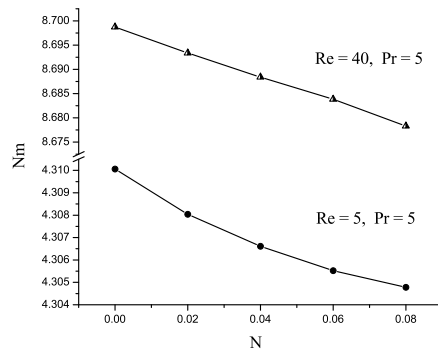
FIG. 4.7. *Mean Nusselt number versus interaction parameter ($N < 0.1$) for aqueous KOH solution ($Pr \approx 5$) when $Re = 5$ and $Re = 40$.*

REFERENCES

[1] I. ATLAS AND K. BURRAGE, *A high accuracy defect-correction multigrid method for the steady incompressible Navier-Stokes equations*, J. Comput. Phys., 114 (1994), pp. 227–233.

[2] L. BARANYI, *Computation of unsteady momentum and heat transfer from a fixed circular cylinder in laminar flow*, J. Comput. Appl. Mech., 4 (2003), pp. 13–25.

[3] J. H. BOYNTON, *Experimental study of an ablating sphere with hydromagnetic effect included*, J. Aerosp. Sci., 27 (1960), p. 306.

[4] A. BRANDT AND I. YAVNEH, *Accelerated multigrid convergence and high-Reynolds recirculation flows*, SIAM J. Sci. Comput., 14 (1993), pp. 607–626.

[5] G. Q. CHEN, Z. GAO, AND Z. F. YANG, *A perturbational h^4 exponential finite difference scheme for convection diffusion equation*, J. Comput. Phys., 104 (1993), pp. 129–139.

[6] S. C. R. DENNIS, J. D. A. WALKER, AND J. D. HUDSON, *Heat transfer from a sphere at low Reynolds numbers,* J. Fluid Mech., 60 (1973), pp. 273–283.

[7] Z. G. FENG AND E. E. MICHAELIDES, *A numerical study on the transient heat transfer from a sphere at high Reynolds and Peclet numbers*, Int. J. Heat Mass Trans., 43 (2000), pp. 219–229.

[8] L. FUCHS AND H. S. ZHAO, *Solution of three-dimensional viscous incompressible flows by a multigrid method*, Internat. J. Numer. Methods Fluids, 4 (1984), pp. 539–555.

[9] U. GHIA, K. N. GHIA, AND K. N. SHIN, *High-Re solutions for incompressible flow using the Navier-Stokes equations and a multigrid method*, J. Comput. Phys., 48 (1982), pp. 387–411.

[10] M. M. GUPTA, *High accuracy solutions of incompressible Navier-Stokes equations*, J. Comput. Phys., 93 (1991), pp. 343–359.

[11] M. M. GUPTA, J. KOUATCHOU, AND J. ZHANG, *A compact multigrid solver for the convection-diffusion equation*, J. Comput. Phys., 132 (1997), pp. 123–129.

[12] ———, *Comparison of second- and fourth-order discretizations for the multigrid Poisson solver*, J. Comput. Phys., 132 (1997), pp. 226–232.

[13] S. R. K. IYENGAR AND R. P. MANOHAR, *High order difference methods for heat equation in polar cylindrical coordinates*, J. Comput. Phys., 72 (1988), pp. 425–438.

[14] M. K. JAIN, R. K. JAIN, AND M. KRISHNA, *A fourth-order difference scheme for quasilinear Poisson equation in polar coordinates*, Comm. Numer. Methods Engrg., 10 (1994), pp. 791–797.

[15] G. H. JUNCU AND R. MIHAIL, *Numerical solution of the steady incompressible Navier Stokes equations for the flow past a sphere by a multigrid defect correction technique*, Internat. J. Numer. Methods Fluids, 11 (1990), pp. 379–395.

[16] J. C. KALITA AND R. K. RAY, *A transformation-free HOC scheme for incompressible viscous flows past an impulsively started circular cylinder*, J. Comput. Phys., 228 (2009), pp. 5207–5236.

[17] S. KARAA AND J. ZHANG, *Convergence and performance of iterative methods for solving variable coefficient convection-diffusion equation with a fourth-order compact difference scheme*, Comput. Math. Appl., 44 (2002), pp. 457–479.

[18] V. N. KURDYUMOV AND E. FERNANDEZ, *Heat transfer from a circular cylinder at low Reynolds numbers*, J. Heat Transfer, 120 (1998), pp. 72–75.

[19] M.-C. LAI, *A simple compact fourth-order Poisson solver on polar geometry*, J. Comput. Phys., 182 (2002), pp. 337–345.

[20] M. LI, T. TANG, AND B. FORNBERG, *A compact fourth-order finite difference scheme for the steady incompressible Navier-Stokes equations*, Internat. J. Numer. Methods Fluids, 20 (1995), pp. 1137–1151.

[21] A. L. PARDHANANI, W. F. SPOTZ, G. F. CAREY, *A stable multigrid strategy for convection-diffusion using high order compact discretization*, Electron. Trans. Numer. Anal., 6 (1997), pp. 211–223.
http://etna.mcs.kent.edu/vol.6.1997/pp211-223.dir

[22] W. E. RANZ AND W. R. MARSHALL, *Evoparation from drops: part I*, Chem. Eng. Prog., 48 (1952), pp. 141–146.

[23] ———, *Evoparation from drops: part II*, Chem. Eng. Prog., 48 (1952), pp. 173–180.

[24] T. V. S. SEKHAR, R. SIVAKUMAR, AND T. V. R. RAVI KUMAR, *Incompressible conducting flow in an applied magnetic field at large interaction parameters*, AMRX Appl. Math. Res. Express, 2005 (2005), pp. 229–248.

[25] T. V. S. SEKHAR, R. SIVAKUMAR, T. V. R. RAVI KUMAR, AND K. SUBBARAYUDU, *High Reynolds number incompressible MHD flow under low R_m approximation*, Int. J. Nonlin. Mech., 43 (2008), pp. 231–240.

[26] M. C. THOMPSON AND J. H. FERZIGER, *An adaptive multigrid technique for the incompressible Navier-Stokes equations*, J. Comput. Phys., 82 (1989), pp. 94–121.

[27] N. UDA, A. MIYAZAWA, S. INOUE, N. YAMAOKA, H. HORIIKE, AND K. MIYAZAKI, *Forced convection heat transfer and temperature fluctuations of lithium under transverse magnetic fields*, J. Nucl. Sci. Technol., 38 (2001), pp. 936–943.

[28] S. P. VANKA, *Block-implicit multigrid solution of Navier-Stokes equations in primitive variables*, J. Comput. Phys., 65 (1986), pp. 138–158.

[29] P. WESSELING, *An Introduction to Multigrid Methods,* Wiley, Chichester, 1992.
[30] S. WHITAKER, *Forced convection heat transfer correlations for flow in pipes, past flat plates, single spheres, and for flow in packed beds and tube bundles*, AIChE J., 18 (1972), pp. 361–371.
[31] T. YOKOMINE, J. TAKEUCHI, H. NAKAHARAI, S. SATAKE, T. KUNUGI, N. B. MORLEY, M. A. ABDOU, *Experimental investigation of turbulent heat transfer of high Prandtl number fluid flow under strong magnetic field*, Fusion Sci. Technol., 52 (2007), pp. 625–629.
[32] J. ZHANG, *Accelerated multigrid high accuracy solution of the convection-diffusion equations with high Reynolds number*, Numer. Methods Partial Differential Equations, 13 (1997), pp. 77–92.
[33] ———, *Numerical simulation of 2D square driven cavity using fourth-order compact finite difference schemes*, Comput. Math. Appl., 45 (2003), pp. 43–52.